Arabian Journal of Chemistry (2016) xxx, xxx–xxx

King Saud University

Arabian Journal of Chemistry

www.ksu.edu.sa
www.sciencedirect.com

ORIGINAL ARTICLE

Copper(II)-oxaloyldihydrazone complexes: Physico-chemical studies: Energy band gap and inhibition evaluation of free oxaloyldihydrazones toward the corrosion of copper metal in acidic medium

Ayman H. Ahmed *, **A.M. Hassan, Hosni A. Gumaa, Bassem H. Mohamed, Ahmed M. Eraky, Ahmed A. Omran**

Department of Chemistry, Faculty of Science, Al-Azhar University, Nasr City, Cairo, Egypt

Received 10 November 2015; accepted 31 May 2016

KEYWORDS

Oxaloyldihydrazone complexes;
Syntheses;
Stereochemistry;
Corrosion inhibition

Abstract A series of oxaloyldihydrazone ligands were prepared essentially by the conventional condensation reaction between oxaloyldihydrazide and different aldehydes e.g., salicylaldehyde, 2-hydroxy-1-naphthaldehyde, 2-hydroxyacetophenone and 2-methoxybenzaldehyde in 1:2 M ratio. The synthesized compounds were purified to give bis(salicylaldehyde)oxaloyldihydrazone ($\mathbf{L_1}$), bis(2-hydroxy-1-naphthaldehyde)oxaloyldihydrazone ($\mathbf{L_2}$), bis(2-hydroxyacetophenone)oxaloyldihydrazone ($\mathbf{L_3}$) and bis(2-methoxybenzaldehyde)oxaloyldihydrazone ($\mathbf{L_4}$). All the oxaloyldihydrazones ($\mathbf{L_1}$–$\mathbf{L_4}$) and their relevant solid copper(II) complexes have been isolated and characterized by various physicochemical techniques. The identity of the synthesized compounds has been ascertained on the basis of elemental analyses, spectral (UV–Vis, IR, ESR, mass, ^{1}H NMR), magnetism and thermal (TG) measurements. The dihydrazones coordinate to the metal center forming binuclear complexes. Upon chelation, the metal center can form a trigonal distorted octahedral structure with $\mathbf{L_1}$ and pseudo tetrahedral configuration with $\mathbf{L_2}$ & $\mathbf{L_3}$ & $\mathbf{L_4}$. The optical band gap energy for all compounds underlies the range of semiconductor materials. The investigated ligands were assayed for their corrosion inhibitive and adsorptive properties on copper surface in 1 M HCl solution using weight loss technique. The results pointed out that, the ligands have a plausible inhibition toward the corrosion of copper specimen. The adsorption reaction on copper surface was found to be spontaneous first

* Corresponding author. Tel.: +20 22629357; fax: +20 22629358.
E-mail address: ayman_haf532@yahoo.com (A.H. Ahmed).

Peer review under responsibility of King Saud University.

Production and hosting by Elsevier

http://dx.doi.org/10.1016/j.arabjc.2016.05.015

order and agreed with physical adsorption mechanism. The adsorption data fitted well to Freundlich, Langmuir and Frumkin adsorption isotherms.

1. Introduction

Despite hydrazones have been under study for a long time owing to their easy preparation, much of their basic chemistry remains unexplored. Hydrazones and their derivatives constitute a versatile class of organic compounds that have interesting biological properties, such as anti-inflammatory, analgesic, anticonvulsant, anti-tumor and anti-HIV (Rollas and Kucukguzel, 2007). Besides, they are important for drug design and organocatalysis and find use as inhibitors and antioxidants (Barbazan et al., 2008). In analytical chemistry, some hydrazones have been utilized as indicators (Berger and Ryan, 1974) and analytical reagent for extraction of trace of copper(II), nickel(II) and cobalt(II) (Odashima et al., 1976; Berger, 1993, 1979). In context of complexation, hydrazones played a central role in the development of coordination chemistry. Hydrazones obtained by the condensation of 2-hydroxy or methoxy aldehydes and ketones with hydrazides are considered potential polynucleating ligands because they have amide, azomethine and phenol or methoxy functions thus offer a variety of bonding possibilities in metal complexes (Sherif and Ahmed, 2010). Nevertheless, a lot of hydrazone-complexes [M = Cu(II), Ni(II), Pd (II), Co(II), Mn(II), V(IV), and ruthenium(II)] have been studied (Hassan et al., 2015), little chelates of oxaloyldihydrazones have been identified (Hassan et al., 2015; Salavati-Niasari and Sobhani, 2008; Lal et al., 2002, 2008). This finding arises from the limited solubility of oxaloyldihydrazones. Examining the solubility of the investigated ligands in common organic solvents illustrated that they are soluble in only DMF and DMSO which indicates that much effort is required to remove solvent traces from the desired products. Interestingly, some hydrazone complexes have been synthesized in zeolite-Y and the resulting materials were inferred by various physicochemical characterization techniques (Ahmed, 2014).

Corrosion of metals is a great problem, faced the world from the last years until now. Despite we can't hide this problem from our life, we can reduce ''inhibit" it in the metals by several methods as the environment need. For this purpose, corrosion inhibitors are employed to react with a metallic surface and thus protect the metal against corrosion especially in acidic environments (Eddy and Odoemelam, 2008). Acid solutions are widely used in industry and the most important fields of application being acid pickling and industrial acid cleaning due to the general aggressiveness of acid solutions; thus enhancing corrosive attack on metallic materials. The most important aspect of inhibition normally considered by corrosion scientists is the relation between molecular structure and corrosion inhibition efficiency (Lorenz and Mansfield, 1985). Indeed, most of the well-known acid inhibitors are organic compounds containing π bonds, phosphorus, sulfur, oxygen and nitrogen as well as aromatic rings in their structure which are the major adsorption centers (Lopez-Sesenes et al., 2011). Heteroatoms such as nitrogen, oxygen and sulfur are capable of forming coordinate covalent bond with metal owing to their free electron pairs and thus acting as inhibitor. Unfortunately, many common corrosion inhibitors employed in aqueous media are health hazards (Flick, 1987).

The present work aims to synthesize and describe four structures of oxaloyldihydrazones and their Cu(II) complexes. The coordination behavior of Cu(II) ions toward the selected oxaloyldihydrazones was studied among them. The study was also accomplished to synthesis of organic compounds (selected hydrazones) able to control the copper dissolution as well as consumption in aggressive acid medium which are widely used for industrial purposes. Checking of these compounds toward the corrosion of copper metal which has important use for pipes, electrical cables, saucepans and radiators,etc., has not been studied yet. In this context the adsorption of all synthesized ligands on copper surface was investigated kinetically and some thermodynamic parameters have been published for first time. Further, the study aims to growing up numbers of semiconductors which may be used as potential materials for harvesting solar radiation in solar cell applications and fabrications of many electronic devices such as microwave ovens, televisions (photograph sensors), radios, watches and telephones, different parts of the PCs, mobiles, sophisticated medical equipment. For this purpose, the energy gap of used ligands and their relevant complexes has been determined to describe their electronic properties.

2. Experimental

2.1. Materials and physical methods

The selected metal salts, diethyl oxalateand hydrazine monohydrate were purchased from Sigma–Aldrich. The employed aldehydes were of E-Merck grade. Oxalic dihydrazide was prepared by the recipe described in Ref. (Hassan et al., 2015), (Exp/Lit. m. p = 240/240 °C). Other chemicals and solvents were of highest purity and used without further purification. Elemental analyses (CHNM), spectral (UV–Vis, FT-IR, ^{1}H NMR, ESR, mass) and thermal (TG) measurements were carried out as reported (Salama et al., 2006; Hassan et al., 2015). Magnetic susceptibility of the samples was measured at room temperature (RT) using Faraday's method where a very small quantity of sample was inserted at the point of maximum gradient (maximum force). The sample is placed in a magnetic field that has a gradient in the vertical direction and the force acting on the sample is determined by using a sensitive balance. The energy (U) of a sample of mass m and magnetic susceptibility χ when kept in horizontal magnetic field H is given by

$$U = -\frac{m\chi H^2}{2}$$

The vertical force F_z exerted on this sample is then given by

$$F_z = m\chi\left(H\frac{d\mathrm{H}}{dz}\right)$$

$$F_z = \Delta mg$$

where Δm is the extra mass measured by the balance due to the force exerted by the field gradient, and g is the acceleration due to gravity (980). The mass susceptibility χ of the sample is given by

$$\chi = \frac{\Delta mg}{mH(\mathrm{d}H/dz)} \quad \text{cgs units}$$

$$\chi_m = \chi \times \mathrm{M.wt}$$

$$H = 1340 \quad \text{at} \quad I = 4\ \mathrm{A} \quad (\mathrm{d}H/\mathrm{d}z) = 173.3 \quad \text{at} \quad I = 4\ \mathrm{A}$$
$$H = 1990 \quad \text{at} \quad I = 6\ \mathrm{A} \quad (\mathrm{d}H/\mathrm{d}z) = 248.8 \quad \text{at} \quad I = 6\ \mathrm{A}$$

where M.wt is the molecular weight of the sample, Δm is the measured pull, m is the sample weight, g is the acceleration due to gravity and H is the coercive field.

Please cite this article in press as: Ahmed, A.H. et al., Copper(II)-oxaloyldihydrazone complexes: Physico-chemical studies: Energy band gap and inhibition evaluation of free oxaloyldihydrazones toward the corrosion of copper metal in acidic medium. Arabian Journal of Chemistry (2016), http://dx.doi.org/10.1016/j.arabjc.2016.05.015

The band gap energy (E_g) of product compounds was calculated from Tauc's equations (Mott and Davis, 1979; Rashad et al., 2013). Copper specimen was of chemical compositions (wt%) depicted in Table 1. Prior to the weight loss experiment, the specimens were polished with emery papers (220–800 grades) until the surface appears free from any scratches and other apparent defects, then washed with distilled water followed by degreasing in absolute ethanol and acetone, dried at room temperature, weighed and finally stored in moisture free desiccators prior to use.

2.2. Preparations

2.2.1. Preparation of oxaloyldihydrazone ligands

The dihydrazone ligands, bis(salicylaldehyde)oxaloyldihydrazone (**L_1**), bis(2-hydroxy-1-naphthaldehyde)oxaloyldihydrazone (**L_2**), bis(2-hydroxyacetophenone)oxaloyldihydrazone (**L_3**) and bis(2-methoxybenzaldehyde)oxaloyldihydrazone (**L_4**), were prepared using the same procedure described in reference Hassan et al. (2015). Oxalicdihydrazide (0.01 mol) dissolved first in hot water (20 cm^3) followed by adding methanol (40 cm^3) was mixed with selected aldehyde [salicylaldehyde, 2-hydroxy-1-naphthaldehyde, 2-hydroxyacetophenone and 2-methoxybenzaldehyde] (0.02 mol) in absolute methanol. The resulting mixture was refluxed for 3 h under constant stirring. The product separated out on concentrating the solution to half of its volume and cooling. The crystals of the desired ligand were collected by filtration through a Buchner funnel and dried in the oven at 50 °C for 2 h. After that the ligand was recrystallized from DMF-$MeOH_{aq}$ mixed solvent, collected, washed thoroughly on filter paper by acetone to remove any excess of dimethylformamide (DMF) and then dried in an electric oven at 50 °C for 4 h. The authenticity of the ligands was proved by elemental analyses in addition to FT-IR, mass and ^{1}H NMR spectroscopy (Tables 2 and 3). The spectral data sustained the chemical structure of the ligands as well as the correct molecular weights.

2.2.2. Preparation of solid complexes

Copper(II) complexes were synthesized by the conventional method reported in reference Hassan et al. (2015). The dihydrazone ligand (1 mmol) was dissolved in a minimum amount of DMF (20 ml) and then 50 ml methanol was added. The resulting solution was added slowly to a methanolic solution of Cu(II) acetate. The resulting mixture was heated under reflux for 4 h and then reduced to 15 cm^3 by evaporation on hot plate. The resulting reaction mixture was cooled down to room temperature and the colored solid complexes were filtered off, washed several times with successive portions of hot solvents (DMF, methanol and acetone, respectively) to remove any excess of unreacted ligand and finally dried in an electric furnace at 80 °C for 7 h.

2.2.3. Weight loss measurement

In the weight loss experiment, 100 ml beakers containing 1 M HCl solutions were employed at room temperature (28 °C). Stock solutions of the inhibitors were prepared in DMF. All test solutions contained 10 ml (20 vol.%) of DMF to maintain inhibitors completely soluble. The total volume of the test solution is 50 ml. The coupons were suspended in the beakers with the aid of glass hooks. In the absence of inhibitors, the coupons were retrieved from their corrodent solutions at 60 min interval for 240 min. Further measurements were carried out after introduction of the additives (**L_1**–**L_4**) at concentrations 5×10^{-4}, 1×10^{-4}, 5×10^{-5} and 1×10^{-5} M in the beaker maintained at the room temperature for the same duration. It is evident that lower concentrations of ligand have been employed to avoid the ligand deposition. Coupons were dipped into saturated ammonium acetate solution at room temperature, to terminate the corrosion reaction. They were washed by scrubbing with a light brush and dried in acetone and finally in an oven maintained at 80 °C. The loss of weight of coupons is evaluated in grams as the difference in weight of the coupons before and after the test (Orubite-Okorosaye and Oforka, 2004).

$$W = W_i - W_f$$

where W = weight loss of coupon, W_i = initial weight of coupon, and W_f = final weight of coupon.

Each reading reported is an average of three experimental readings recorded to the nearest 0.0001 g on an Adam184 electronic weighing balance. The value of corrosion rate, ρ (in g cm^{-2} min^{-1}) was calculated from the following equation (Mohammed-Dabo et al., 2011):

$$\rho = \frac{W}{A \times t}$$

where W = weight loss to the nearest 0.0001 g, A = area of specimen to the nearest 0.01 cm^2 (2 × area of one surface/face) and t = exposure time (minutes).

The percentage inhibition efficiency (%IE), and a parameter surface coverage (θ) which represents the part of the surface covered by the inhibitor molecules, were calculated using the following equations (Mohammed-Dabo et al., 2011):

$$\eta\% = \left[1 - \frac{\rho_1}{\rho_2}\right] \times 100\%$$

$$\theta = 1 - \frac{\rho_1}{\rho_2}$$

where η% = corrosion inhibition efficiency, ρ_1 = corrosion rate in the presence of inhibitors, ρ_2 = corrosion rate in the absence of inhibitor at the same temperature and θ = surface coverage.

2.2.4. Kinetic treatment of weight loss results

Spontaneous corrosion reaction is a heterogeneous one, composed of anodic and cathodic reactions with the same rate.

Table 1 Characteristic specifications for copper coupons used for weight loss measurements.

Specimen	C	Si	As	Sn	Mn	P	S	Cr	Ni	Pb	Zn	Cu	Al	Fe
Copper	–	–	0.005	0.001	–	0.017	–	–	0.01	0.005	0.281	Balance	–	0.019

Please cite this article in press as: Ahmed, A.H. et al., Copper(II)-oxaloyldihydrazone complexes: Physico-chemical studies: Energy band gap and inhibition evaluation of free oxaloyldihydrazones toward the corrosion of copper metal in acidic medium. Arabian Journal of Chemistry (2016), http://dx.doi.org/10.1016/j.arabjc.2016.05.015

Table 2 Analytical, physical and spectroscopic data of the oxaloyldihydrazones and their copper(II) complexes.

Compd./symbol	M.p (°C)	Found (cald.)%				^{1}H NMR	$\mu_{eff.}$	M^+	E_g	$g_\perp$	$g_{//}$	$g_{av.}$
	Color	C	H	N	M	Chemical shift (δppm)	4 A/6 A	Found/calcd.	(eV)			
$C_{16}H_{14}N_4O_4$/**L_1**	> 300	59.1	5.4	16.2	–	12.6(NH, s), 10.98(OH, s), 8.75(CH=N, s)	–	326.0/326.0	2.88	–	–	–
	Yellow	(58.9)	(4.3)	(17.2)	–	6.6–8.40 (aromatic protons, m)						
$C_{24}H_{18}N_4O_4$/**L_2**	> 300	68.1	5.3	12.9	–	12.76(NH, s), 12.57(OH, s), 9.74(CH=N, s)	–	427.1/426.4	2.46	–	–	–
	Yellow	(67.7)	(4.3)	(13.2)	–	7.0–8.8 (aromatic protons, m)						
$C_{18}H_{18}N_4O_4$/**L_3**	> 300	59.5	6.1	14.7	–	12.85(NH, s), 11.85(OH, s), 6.6–8.0 (aromatic protons, m)	–	356.4/354.2	2.78	–	–	–
	Pale Yellow	(61)	(5.1)	(15.8)	–	2.48(CH_3, s)						
$C_{18}H_{18}N_4O_4$/**L_4**	> 300	59.2	5.8	15.7	–	12.3(NH, s), 11.9(OH, s), 8.95(CH=N, s)	–	355.0/354.4	3.05	–	–	–
	White	(61)	(5.1)	(15.8)	–	6.8–8.5 (aromatic protons, m), 3.93(OCH_3, s)						
$[Cu_2(L_1\text{-}3H)(H_2O)_6]\cdot OAc\cdot 2H_2O$/**I**	> 300	33.8	4.9	8.8	20.4	–	1.9/1.8	–	2.10	1.99	2.11	1.36
	Brown	(33.1)	(4.6)	(8.6)	(19.5)							
$[Cu_2(L_2\text{-}3H)(OAc)(H_2O)]\cdot 2H_2O$/**II**	> 300	46.8	3.4	8.1	19.1	–	1.9/1.7	–	1.78	1.89	2.01	1.93
	Brick Red	(47.1)	(3.6)	(8.4)	(19.2)							
$[Cu_2(L_3)(OAc)_4]\cdot 3H_2O$/**III**	> 300	40.0	4.3	7.0	16.4	–	1.8/1.6	–	2.12	–	–	–
	Green	(40.5)	(4.7)	(7.3)	(16.5)							
$[Cu_2(L_4)(OAc)_4]\cdot 2H_2O$/**IV**	> 300	41.1	4.2	7.1	17.8	–	1.7/1.4	–	1.90	195	2.06	1.99
	Brown	(41.4)	(4.5)	(7.4)	(16.8)							

On this basis the kinetic analysis of the data is considered necessary. In the present study, the initial weight of steel coupon at time, t is designated W_i, the weight loss is ΔW and the weight change at time t is $(W_i - \Delta W)$ or W_f. When $\log W_f$ was plotted against time, a linear variation was observed, which confirms a first order reaction kinetics with respect to copper in HCl solutions, formulated as (Okafor et al., 2010)

$$\log W_f = \log W_i - Kt$$

where W_i = the initial weight before immersion, K = slope (the rate constant), and t is time.

From the rate constant values obtained from the graphs, regarding the adsorption reaction on copper surface proceeds as first order, the half-life values (t_o) of the metal in the test solutions were calculated using the following equation (Okafor et al., 2010):

$$t_{1/2} = \frac{\ln 2}{K} = \frac{0.693}{K}$$

3. Results and discussion

Oxaloyldihydrazones (**L_1**–**L_4**) and their solid Cu(II)-complexes have been isolated in pure form. Physical, analytical and spectroscopic data of the hydrazones and their isolated copper(II) complexes are summarized in Tables 2 and 3. The complexes are air stable for long time and insoluble in MeOH/EtOH, Et_2O, $CHCl_3$, acetone, CCl_4 as well as benzene. Complexes **I**–**III** are soluble in dimethylformamide (DMF) and dimethylsulfoxide (DMSO) while complex **IV**is partially soluble in the abovementioned solvents. Comparison of the elemental analysis for both the calculated and found percentages deduced the compositions and the proposed formulae of the isolated complexes.

3.1. Chemical structures of dihydrazones and their Cu^{II}-complexes

3.1.1. IR spectra and bonding

The positions of the significant IR bands of dihydrazones and their copper complexes are recorded in Table 3 and clarified by Fig. 1.

Ligands: oxloyldihydrazones (**L_1**–**L_4**) can exist either in the trans(staggered) configuration or in cis-configuration, Fig. 2, (Hassan et al., 2015). In cis-configuration, the dihydrazone can adopt either anti-cis-configuration or syn-cis-configuration. Infrared spectra gave strong bands at 1602–1617 cm^{-1} assignable to the azomethine group ($\nu_{C=N}$). The observation of these bands is unambiguously confirmation of the interaction of dihydrazides with aldehydes forming azomethine linkages. The bands of $\nu(OH)_{phenolic/naphthoic}$, ν(NH) and ν(C=O) for **L_1**–**L_3** were noticed at 3149, 3204 and 1666;3476, 3166 and 1705(m) + 1660(v.s); and 3448, 3293 and 1689(m) + 1651(v.s) cm^{-1}, respectively. Meanwhile, **L_4** which does not contain o-hydroxy group revealed ν(NH) at 3202 cm^{-1} and ν(C=O) at 1653 cm^{-1}. The appearance of both ν(C=O) and ν(NH) simultaneously in the IR spectra of **L_1**–**L_4** indicates the presence of keto forms. The observation of carbonyl groups (C=O) near 1660 cm^{-1} as one band in case of **L_1** and **L_4** and pair of bands near 1660 and

Please cite this article in press as: Ahmed, A.H. et al., Copper(II)-oxaloyldihydrazone complexes: Physico-chemical studies: Energy band gap and inhibition evaluation of free oxaloyldihydrazones toward the corrosion of copper metal in acidic medium. Arabian Journal of Chemistry (2016), http://dx.doi.org/10.1016/j.arabjc.2016.05.015

Table 3 Significant IR and electronic absorption data of oxaloyldihydrazones and their copper(II) complexes.

Symbol	ν(OH)	ν(H_2O) phenolic (enolic)	ν(NH)	ν(C—H)	ν(C=O) aromatic (aliphatic)	ν(C=N)	ν(C—O) phenolic	ν(C—OMe)	ν(C=C)	δ(C—H) aromatic out of plane	ν(M—O) phenolic/enolic (carbonyl/methoxy)	λ_{max}, nm (assignments)
L_1	3149 (3278)	–	3204	3062 (2924)	1666	1620	1275	–	1403 1458 1486	756	–/– (–/–)	387(n–π*, C=N), 372(n–π*, C=O), 340(π–π*, C=N), 300 (π–π*, C=O), 288(π–π*, phenyl)
L_2	3476 (–)	–	3166	3043 (2926)	1705 1660	1621	1287	–	1465 1541 1574	741	–/– (–/–)	395(n–π*, C=N), 390(n–π*, C=O), 370(π–π*, C=N), 348 (π–π*, C=O), 320(π–π*, phenyl)
L_3	3448 (–)	–	3293	3048 (2923)	1689 1651	1607	1246	–	1449 1486 1512	746	–/– (–/–)	378(n–π*, C=N), 348(n–π*, C=O), 322(π–π*, C=N), 300 (π–π*, C=O), 280(π–π*, phenyl)
L_4	– (3227)	–	3202	3041 (2940)	1653	1600	–	964	1464 1486 1572	760	–/– (–/–)	371(n–π*, C=N), 345(n–π*, C=O), 320(π–π*, C=N), 290 (π–π*, C=O), 270(π–π*, phenyl)
I	– (–)	3419	3250	3053 (2924)	1655	1609 1600	1309	–	1466	756	598/483 (–/–)	666 ($^2Eg \rightarrow {}^2T_2g$) 470(L → MCT)
II	– (–)	3418	3260	3054 (2923)	1650	1616 1602	1300	–	1452 1535	747	546/489 (–/–)	725 ($^2B_2 \rightarrow {}^2E$) 500(L → MCT)
III	3320 (3356)	3530	3293	3075 (2925)	1670	1631 1605	1300 1235	–	1468 1549	749	560/480 (–/–)	700 ($^2B_2 \rightarrow {}^2E$) 420(L → MCT)
IV	– (3350)	3445	3202	3040 (2930)	1645	1600	–	980	1465 1539	752	–/490 (–/522)	750 ($^2B_2 \rightarrow {}^2E$) 440(L → MCT)

Please cite this article in press as: Ahmed, A.H. et al., Copper(II)-oxaloyldihydrazone complexes: Physico-chemical studies: Energy band gap and inhibition evaluation of free oxaloyldihydrazones toward the corrosion of copper metal in acidic medium. Arabian Journal of Chemistry (2016), http://dx.doi.org/10.1016/j.arabjc.2016.05.015

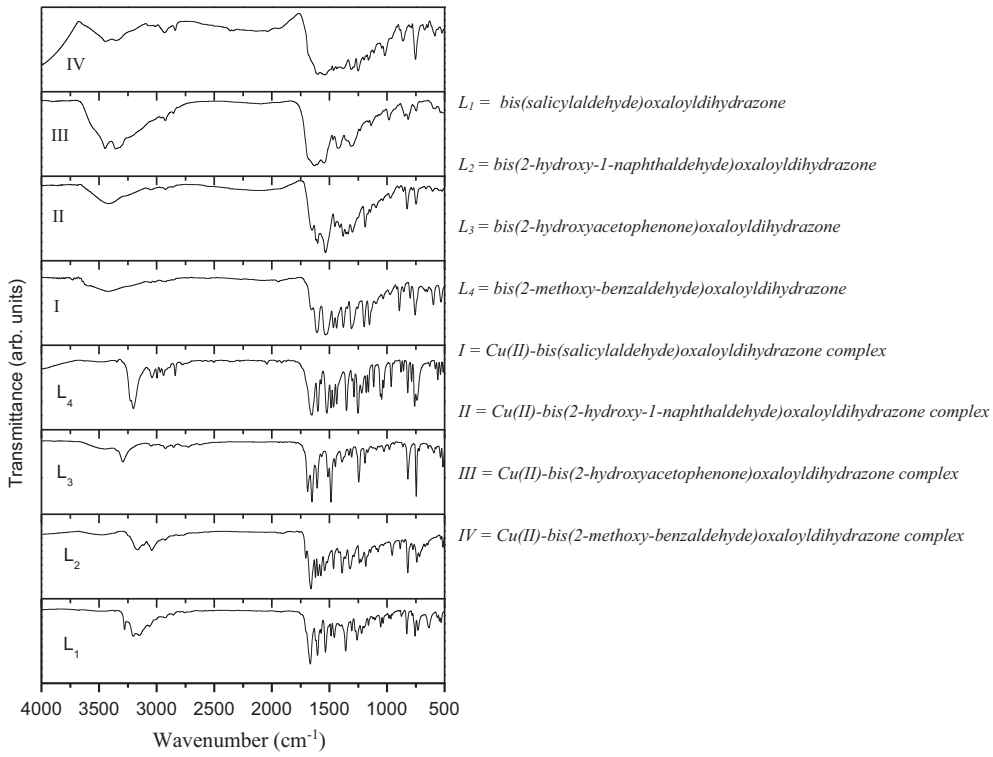

Figure 1 IR spectra of oxaloyldihydrazones and their copper(II) complexes.

1700 cm^{-1} for each $\mathbf{L_2}$ and $\mathbf{L_3}$ indicates the trans (staggered-structure, Fig. 2) configuration for $\mathbf{L_1}$ and $\mathbf{L_4}$ while mixture of [cis(syn/anti-cis-structure) + trans(staggered-structure), Fig. 2] isomers is for $\mathbf{L_2}$ and $\mathbf{L_3}$. This suggestion results from the field effect phenomenon which can be elucidated as follows. When the two carbonyl (C═O::) groups are in the same direction (cis configuration), the non-bonding electrons present on oxygen atoms cause electrostatic repulsion. This causes a change in the state of hybridization belongs to C═O group and also makes it to go out the plane of the double bond. Thus, the configuration diminished and absorption occurs at higher wave number. Subsequently, cis is absorbed (due to the field effect) at higher frequency compared to trans isomer. Subsequently, $\mathbf{L_2}$ and $\mathbf{L_3}$ showed two bands for C═O, one of them (at high frequency) associated with syn/anti-cis-symmetry while that at lower frequency related to staggered configuration. The low intensity of high frequency bands (near 1700 cm^{-1}) compared with that at low frequency (near 1660 cm^{-1}) indicates the domination of staggered structure. Worthy mention, NMR spectroscopy provided satisfactory agreement with this suggestion as shown later. The observation of OH (phenolic) group in $\mathbf{L_1}$ at lower position (3149 cm^{-1}) is taken as evidence to the persistence of intramolecular H-bonding between the phenolic-OH and azomethine group (O─H···N) Mohammed-Dabo et al., 2011. The proposition of intermolecular H-bond (O─H···O─H) between ligand molecules is excluded owing to the sharpness of this band. The remarkable downward frequency shift indicates the strength of this bond. In fact, ^{1}H NMR did not distinguish this H-bond in its spectra because execution of NMR analysis in high polar solvent (DMSO) led to break these bonds. The phenolic-OH group did not form H-bonding in case of ligands $\mathbf{L_2}$ and $\mathbf{L_3}$ where it is observed after 3400 cm^{-1}. Further, the existence of two bands at 3278 cm^{-1} ($\mathbf{L_1}$) and 3227 cm^{-1} ($\mathbf{L_4}$) may be attributed to $\nu(OH)_{enolic}$ in H-bond bonding with azomethine group. The negative shift of these two bands compared with their normal positions asserts the weakness of this bond. Apparently the obscure of enolic OH in NMR spectra of $\mathbf{L_1}$ and $\mathbf{L_4}$ is attributed to two factors: (1) its lower concentrations,in which minute molecules may change one or two of its C═O groups into enolized configuration but the keto form is still dominated, (2) dilution by high polar DMSO disrupted these H-bonds returning the modified molecules into keto forms. The significant ν(C─O) groups associated with the aromatic ring of the dihydrazones $\mathbf{L_1}$–$\mathbf{L_4}$ were observed at 1275, 1287, 1246 and 964 cm^{-1}, respectively (Mohammed-Dabo et al., 2011). In addition to the above, all the ligands showed 3–4 bands in the range 1400–1600 cm^{-1} related to ν(C═C) of the aromatic ring. Also, each ligand exhibited strong band in the region 700–800 cm^{-1} corresponding to the out of plane deformation of the aromatic ring. The positions of other bands assigned to $\upsilon(CH)_{aliphatic}$ near 2900 cm^{-1} and $\upsilon(CH)_{aromatic}$ near 3050 cm^{-1} are demonstrated in Table 3.

Cu(II) complexes: The IR spectra of the Cu^{II}–$\mathbf{L_1}$–$\mathbf{L_4}$ complexes are represented in Fig. 1, meanwhile the assignment of the significant IR bands is depicted in Table 3. Indeed, it is difficult to unambiguously assign the bands due to foundation of various groups e.g., C═O, C═N, N─C═O, NH, OH, ph ring, C─N and C─H which absorb in the overlapping regions. On examining the IR spectra of the complexes in comparison with those of the free ligands, in these complexes, the dihydrazones ($\mathbf{L_1}$–$\mathbf{L_4}$) behave as tetra- and hexa-dentate ligands

Please cite this article in press as: Ahmed, A.H. et al., Copper(II)-oxaloyldihydrazone complexes: Physico-chemical studies: Energy band gap and inhibition evaluation of free oxaloyldihydrazones toward the corrosion of copper metal in acidic medium. Arabian Journal of Chemistry (2016), http://dx.doi.org/10.1016/j.arabjc.2016.05.015

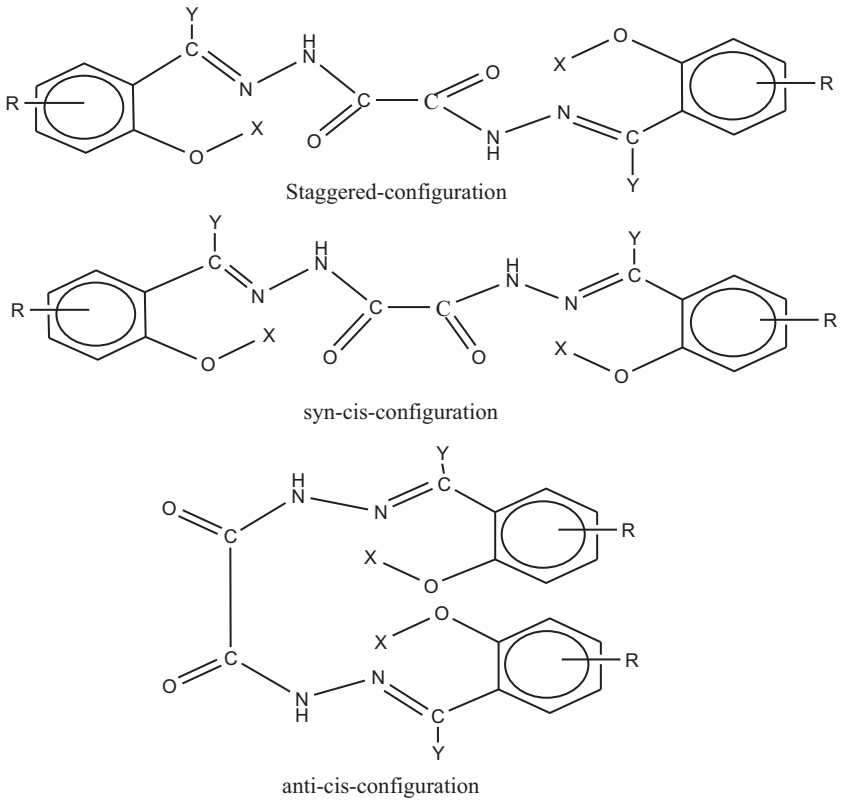

Figure 2 Proposed structures of oxaloyldihydrazone ligands, where L_1 (R = H, X = H, Y = H), L_2 (R = ph, X = H, Y = H), L_3 (R = H, X = H, Y = CH_3) and L_4 (R = H, X = CH_3, Y = H).

toward two centered copper(II) ions forming stable five or six membered chelate rings around each metal ion. This tremendous behavior of ligands can be explained by the aid of IR data as follows:

For **I** and **II** (In comparison with free corresponding ligands) the mode of bonding is proposed on the following basis: (1) The splitting (1616, 1612 cm^{-1}, complex **II**) or broadening (1609, 1600 cm^{-1}, **I**) of the azomethine group suggested the involvement of this group in bonding (Hassan et al., 2007) considering two dissimilar azomethine groups (Okafor et al., 2010). One of these C═N groups is coordinated with copper (II) ion while the other is free. This happened due to the enolization of left or right half of the dihydrazone molecule assuming keto-enol skeleton. (2) The weakness of NH (shoulder) and C═O bands accompanied with changes in their locations is most probable due to the obscure of one NH and one C═O group by virtue of enolization. Foundation of C═O as one band in **II** instead of two bands in free $\mathbf{L_2}$ besides its absorption at somewhat lower frequency is most probable due to the presence of the two oxygen atoms related to the carbonyl groups in (a) trans direction because of the field effect, or (b) cis direction but with occupation of the free electrons on oxygen by coordination with the central metal. In fact, magnetic data (shown later) supported the second probable for high spin **II** complex considering that quenching of the spin moments of the copper ions (spin coupling) leads to decrease the μ_{eff} value. (3) Unnoticeable of the ν(OH) of o-hydroxyl group supported deprotonation of the above group through the coordination. This result is evidenced by the appearance of new bands attributed to $\nu(M{-}O_{phenolic/naphthoic})$ as well as the positive shift observed for ν(C─O) vibrations (Mohammed-Dabo et al., 2011; Abd El-Wahab et al., 2015).

For **III** (in comparison with free $\mathbf{L_3}$), the mode of bonding is proposed on the following basis: (1) The splitting of the azomethine group (1607 → 1605, 1631 cm^{-1}) suggested the involvement of this group in bonding (Mohammed-Dabo et al., 2011) assuming the existence of coordinated and uncoordinated azomethine groups. As previously clarified, this occurred due to keto-enol skeleton. (2) The weakness of NH (3293 cm^{-1}, weak shoulder) and C═O (1670 cm^{-1}, medium) bands is most probably due to the obscure of one NH and one C═O group by virtue of enolization. Also, persistence of C═O as one band in **III** instead of two bands in free $\mathbf{L_3}$ coincides with the presence of the two oxygen atoms related to the carbonyl groups in cis direction but with occupation of the free electrons on oxygen by coordination with the central metal. As mentioned in **II**, magnetic data coincide with the second probable for high spin **III** complex considering a quenching of the spin moments of the copper ions. (3) Observation of the ν(OH) phenolic as two bands (3447, 3320 cm^{-1}) instead of one band in $\mathbf{L_3}$ (3448 cm^{-1}) referred to the existence of two kinds of phenolic OH suggesting coordinated and free OH group. This probable is endorsed by foundation of $\nu(M{-}O_{phenolic})$ at 560 cm^{-1} and splitting of νC─O (phenolic) at 1300, 1235 cm^{-1}. Moreover, existence of OH enolic at 3356 cm^{-1} illustrated that deprotonation of this group did not occur. This conclusion is evidenced by the appearance of new band assignable to $\nu(M{-}OH_{enolic})$ at 480 cm^{-1} (Kumar et al., 2011).

In case of **IV**, half of the $\mathbf{L_4}$ molecule was altered to enol form and coordination with two metal ions took place via

Please cite this article in press as: Ahmed, A.H. et al., Copper(II)-oxaloyldihydrazone complexes: Physico-chemical studies: Energy band gap and inhibition evaluation of free oxaloyldihydrazones toward the corrosion of copper metal in acidic medium. Arabian Journal of Chemistry (2016), http://dx.doi.org/10.1016/j.arabjc.2016.05.015

two OMe, one C═O, and one protonated enolized carbonyl (C─OH) groups. This behavior is assumed on the basis: (a) the observation of ν(NH) and ν(C═O) at the same locations but with weak intensity indicates that half of **L_4** molecule was enolized. The positive shift of ν(C─OMe) with its appearance as one band illustrated the coordination of methoxy group with Cu(II) ion. The observation of ν(C═N) at the same position (1600 cm^{-1}) without any shift elucidated that C═N group did not contribute in bonding. The broadening of this band may be due to the interference absorption of various kinds of C═N groups (Salapathy and Sahoo, 1970).

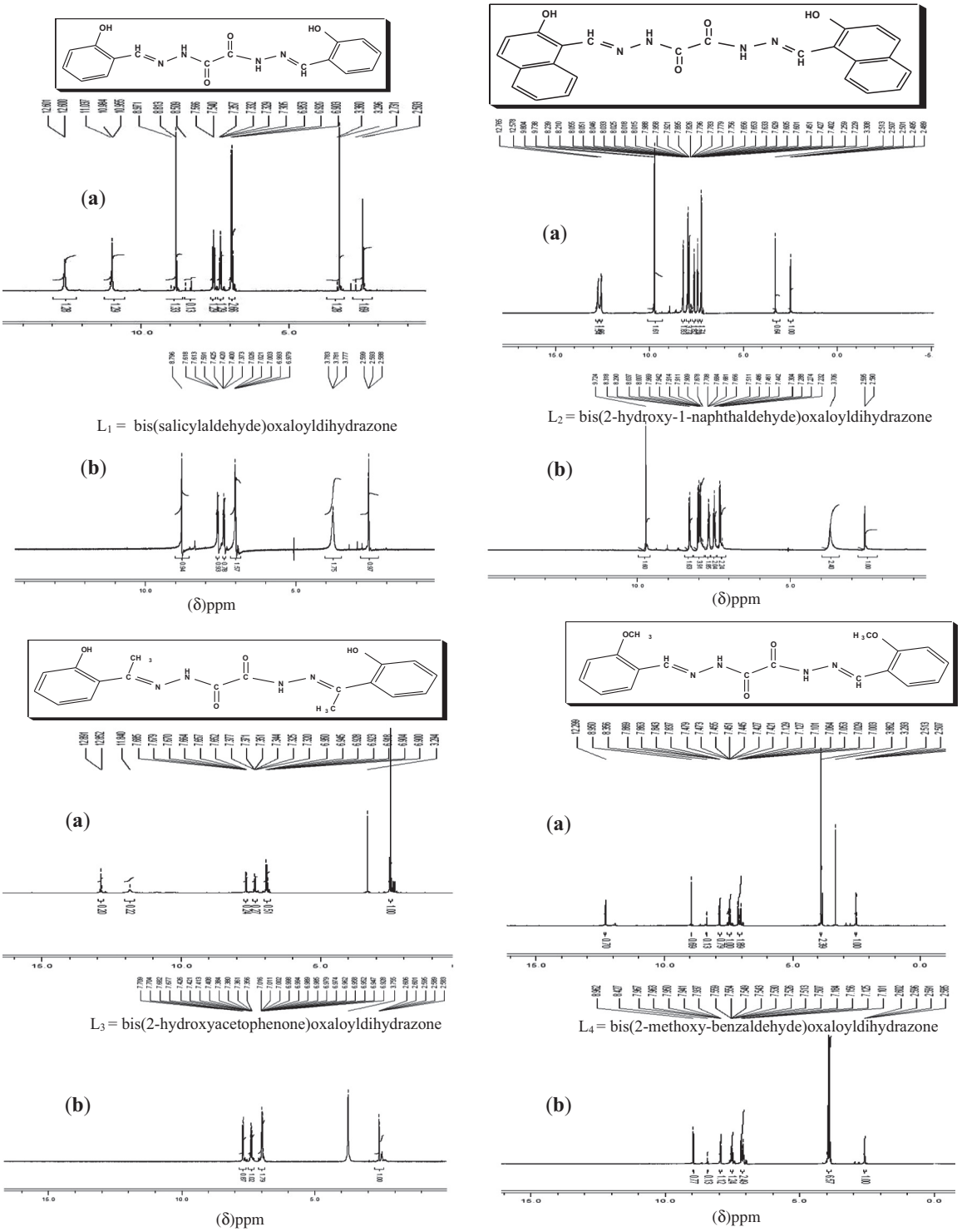

Figure 3 ^1H NMR spectra of the oxaloyldihydrazones in (a) DMSO d_6 and (b) DMSO d_6 + D_2O.

Doubtless, the appearance of new M—O bands in all copper complexes (Table 3) gives a clue to the formation of discrete complexes. Strong broad absorptions in the 3300–3550 cm^{-1} region for metal complexes substantiated the presence of crystalline and coordinated water in all copper species. Other bands ascribed to negative acetate ion (OAc) were located at 1345–1381 and 1410–1440 cm^{-1}, respectively, suggesting ν_{as} and ν_s carboxylic modes. The larger separation between the ν_{as} and ν_s frequencies confirmed the coordination of acetate as a unidentate anion through the C—O moiety of the carboxylic group (Nakamoto, 1970). Also, the slight changes in the positions of $\nu(C{=}C)_{ph}$ upon chelation are mainly due to metal–ligand interaction.

3.1.2. ^1H NMR spectra

The assignment of the main signals in ^1H NMR spectra of all ligands (Hassan et al., 2015) is shown in Fig. 3 along with Table 1, where copper complexes have not been scanned owing to their paramagnetic nature. ^1H NMR spectra of all ligands exhibited multiple signals of the aromatic protons in the 6.5–8.5 ppm region. The signals of equal integration observed in **L_1, L_2** and **L_3** at δ (12.6, 11), (12.8, 12.6) and (12.9, 11.8) ppm downfield of TMS have been assigned to NH and ortho-OH protons, respectively. On the other hand, **L_4** revealed a signal at 12.3 ppm attributed to secondary NH group. Upon the addition of D_2O then OH and NH signals were obscured. Further, the existence of the δOH (phenolic/naphthoic) at its normal frequency excluded any intramolecular hydrogen bonding operating between ortho-OH and CH═N group (CH═N···H—O). The azomethine signals, δ(CH═N), observed only in **L_1, L_2** and **L_4** have been assigned at 8.75, 9.73 and 8.95 ppm, respectively. As reported in the literature (Kumar et al., 2011), if the dihydrazone exists in the syn-cis-configuration or staggered configuration, the δOH, δNH and δCH═N, resonances, each should appear as a singlet. However, the appearance of these signals in the form of six signals (doublet of doublet) indicates anti-cis (chair) configuration. Actually, the features of the ^1H NMR spectra of the dihydrazones are compatible with syn-cis- or staggered symmetry. According to IR interpretation mentioned above, the staggered configuration is well defined/dominated for all ligands (**L_1–L_4**). ^1H NMR spectra of **L_3** and **L_4** differ from other ligands spectra where they showed signals at 2.55 and 3.9 ppm downfield of TMS due to the methyl (CH_3) and methoxy (OCH_3) protons, respectively (Sherif and Ahmed, 2010; Hassan et al., 2015; Nakamoto, 1970).

3.1.3. Electronic spectra

The assignments of the observed electronic absorption bands of the oxaloylhydrazones and their metal complexes in Nujol mull (Sutton, 1968; Lever, 1984) as well as the magnetic data of the formed chelates are depicted in Table 3.

The electronic data of the studied ligands exhibited five absorption bands at λ_{max} (nm) equals 371–395 (n–π*, C═N), 345–390 (n–π*, C═O), 320–370 (π–π*, C═N), 290–348 (π–π*, C═O) and 270–320 (π–π*, aromatic ring) (Ahmed et al., 2015).

Spectrum of **I** showed an absorption band at 666 nm suggesting a trigonal distorted octahedral structure. Meanwhile, each of other complexes (**II–IV**) exhibited an absorption band within the range 700–750 nm which is taken as a conclusive evidence for the pseudo tetrahedral environment. The band observed at 420–500 nm for **I–IV** is mainly assigned to charge-transfer L → Cu on the basis of its high intensity. This ligand–metal charge transfer (L → MCT) transition may be associated with, most probably, an electronic excitation from the HOMO of ortho phenolate/naphtholate/methoxy oxygen to the LUMO of copper(II) ion Sutton, 1968. Any band due to d-d transition in this region is masked by this charge transfer transition band.

For the obtained magnetic studies, the values of μ_{eff} at room temperature (Table 2) for the consequential binuclear copper (II) complexes (**I–IV**), the magnetic moment values are less than those expected per molecular formula regarding the existence of two metal ions in the proposed structures. This can be explained on the basis of metal–metal interaction. It is suggested that these complexes have high spin but presence of two metals near to each other in the same molecule may cause partial quenching of the spin moments of the metal ions (spin coupling) decreasing the magnetism (Mahapatra et al., 1991). This means that the supposition of two metal ions in the molecular structure is not excluded and the obtained μ_{eff} values may be not conflicted with the proposed structures.

3.1.4. TG studies of Cu(II)-complexes

Thermal stability of all investigated complexes **(I–IV)** was studied.

The TGA data of complex (**I**), revealed six stages of decomposition. The first stage (50–90 °C) related to the loss of (found/calculated = 4.7/5.5)% of the original weight of

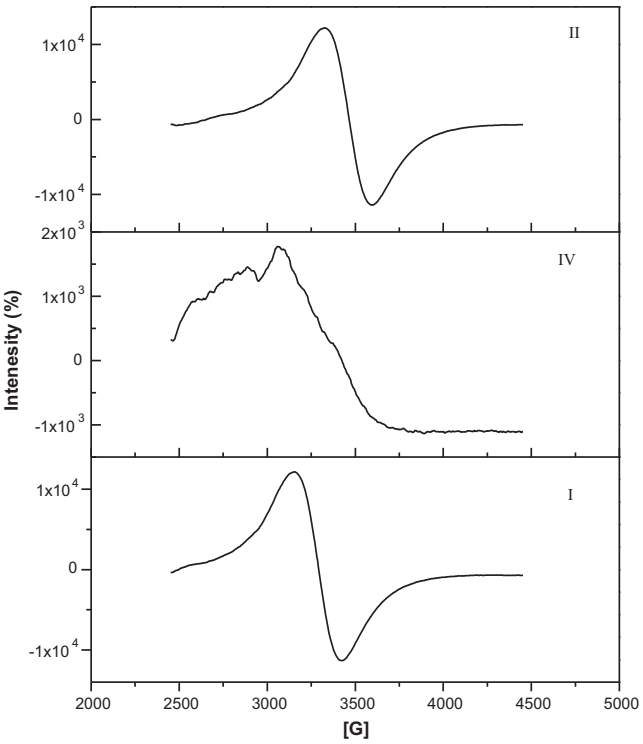

I = Cu(II)-bis(salicylaldehyde)oxaloyldihydrazone complex,

II = Cu(II)-bis(2-hydroxy-1-naphthaldehyde)oxaloyldihydrazone complex and

IV = Cu(II)-bis(2-methoxy-benzaldehyde)oxaloyldihydrazone complex

Figure 4 Suggested structures of the Cu^{II}-oxaloyldihydrazone complexes.

Please cite this article in press as: Ahmed, A.H. et al., Copper(II)-oxaloyldihydrazone complexes: Physico-chemical studies: Energy band gap and inhibition evaluation of free oxaloyldihydrazones toward the corrosion of copper metal in acidic medium. Arabian Journal of Chemistry (2016), http://dx.doi.org/10.1016/j.arabjc.2016.05.015

complex corresponding to the loss of two crystalline water molecules. The second step of degradation (90–170 °C) corresponds to the elimination of one acetate group (found/calculated% = 7.7/8.7). After the last step of decomposition (700–800 °C), a residue of $2CuCO_3$ was formed (found/calculated% = 36.8/37.8).

The TGA data of complex (**II**) exhibited five stages of disintegration. The first stage corresponds to expelling of two crystalline water molecules (found/calculated = 5.6/5.4)% at the temperature range 50–110 °C. The second step of decomposition corresponds to the loss of (found/calculated = 9.1/8.6)% within the range (175–230 °C) which can be attributed to the loss of one coordinated acetate group. The third stage (230–275 °C) corresponds to the loss of coordinated water molecule (found/calculated% = 3.6/2.7). After that, a residue of (36.5/37.2)% of the original weight of the complex was observed which corresponds to the loss of $2CuCO_3$ molecules.

The TGA curve of the complex **III** showed three steps of decomposition. The first step observed at 50–140 °C corresponds to the elimination of three crystalline water molecules (found/calculated% = 7/8). The second step observed in the range 140–330 °C refers to expelling of four acetate groups (found/calculated% = 29.4/29.6). After that, a residue of (found/calculated = 33.8/32.0)% of the original weight of the complex was obtained assigned to $2CuCO_3$ molecules.

The TGA curve of **VI** complex exhibited four stages of decomposition started at 50, 150, 300, and 400 °C. The first stage (50–150 °C) corresponds to the loss of two crystalline water (found/calculated = 4/4.8)%. The other three steps of decomposition point to the gradual disintegration of the complex. At the final step, a residue of $CuCO_3$ and CuO mixture (found/calculated = 27/26)% was formed.

3.1.5. ESR spectra

The ESR spectra of complexes **I**, **II** and **IV** showed broad signals (Fig. 4) with two "g" values ($g_{//}$, $g_{\perp}$) depicted in Table 2. The spectra of I and II have symmetrical shape while IV is not. For all complexes the $g_{//} > g_{\perp} > 2.0023$, characteristic of complexes with $^2B_1(d_{x^2-y^2})$ orbital ground state. The average g values were calculated according to the following equation:

$$g_{av.} = \frac{1}{3[g_{//} + 2g_{\perp}]}$$

where the calculated values are presented also in Table 2. The $g_{//}$ is a moderately function for covalent nature.

I, **II** and **IV** complexes exhibited $g_{//}$ at 1.36, 1.93 and 1.99, respectively which are less than 2.3, suggesting covalent character of copper–ligand bonds in the present complexes, where, $g_{//} > 2.3$ concerns to ionic metal–ligand bond (Lever, 1984; Kivelson and Nieman, 1961). Fairly high values of g are in conformity with the oxygen and nitrogen coordination in these compounds (Lal et al., 2008). The splitting in case of IV bands may be due to the additional interactions of the magnetic moment of the electron with local magnetic fields originating from non-zero nuclear spins. This coupling is

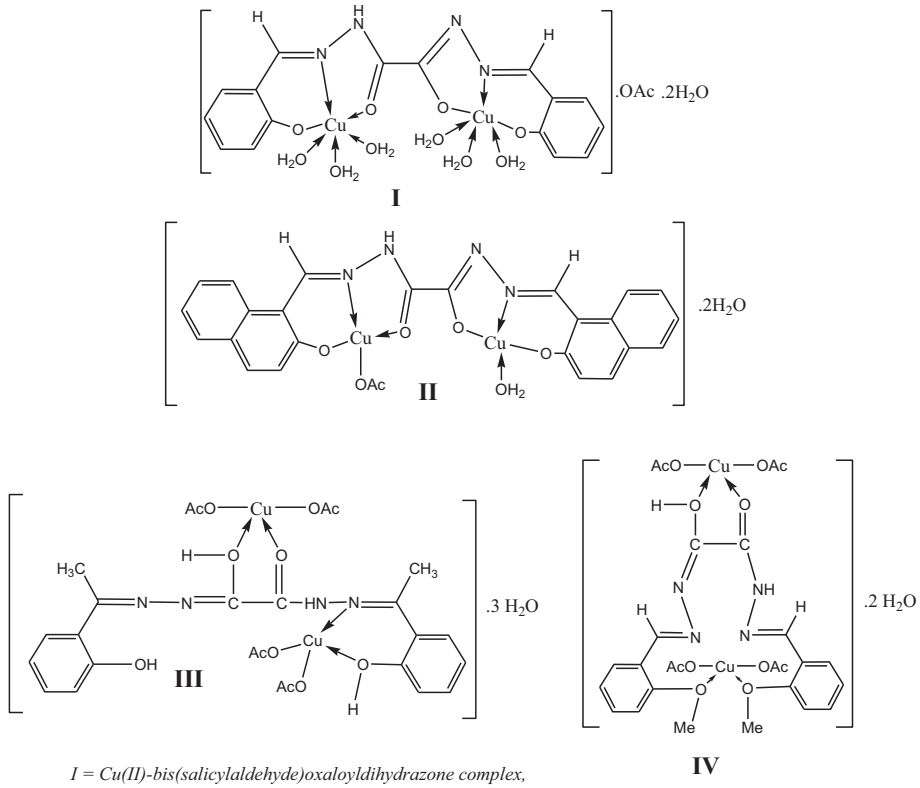

I = Cu(II)-bis(salicylaldehyde)oxaloyldihydrazone complex,

II = Cu(II)-bis(2-hydroxy-1-naphthaldehyde)oxaloyldihydrazone complex

III = Cu(II)-bis(2-hydroxyacetophenone)oxaloyldihydrazone complex

IV = Cu(II)-bis(2-methoxy-benzaldehyde)oxaloyldihydrazone complex

Figure 5 ESR spectra of solid Cu^{II}-oxaloyldihydrazone complexes.

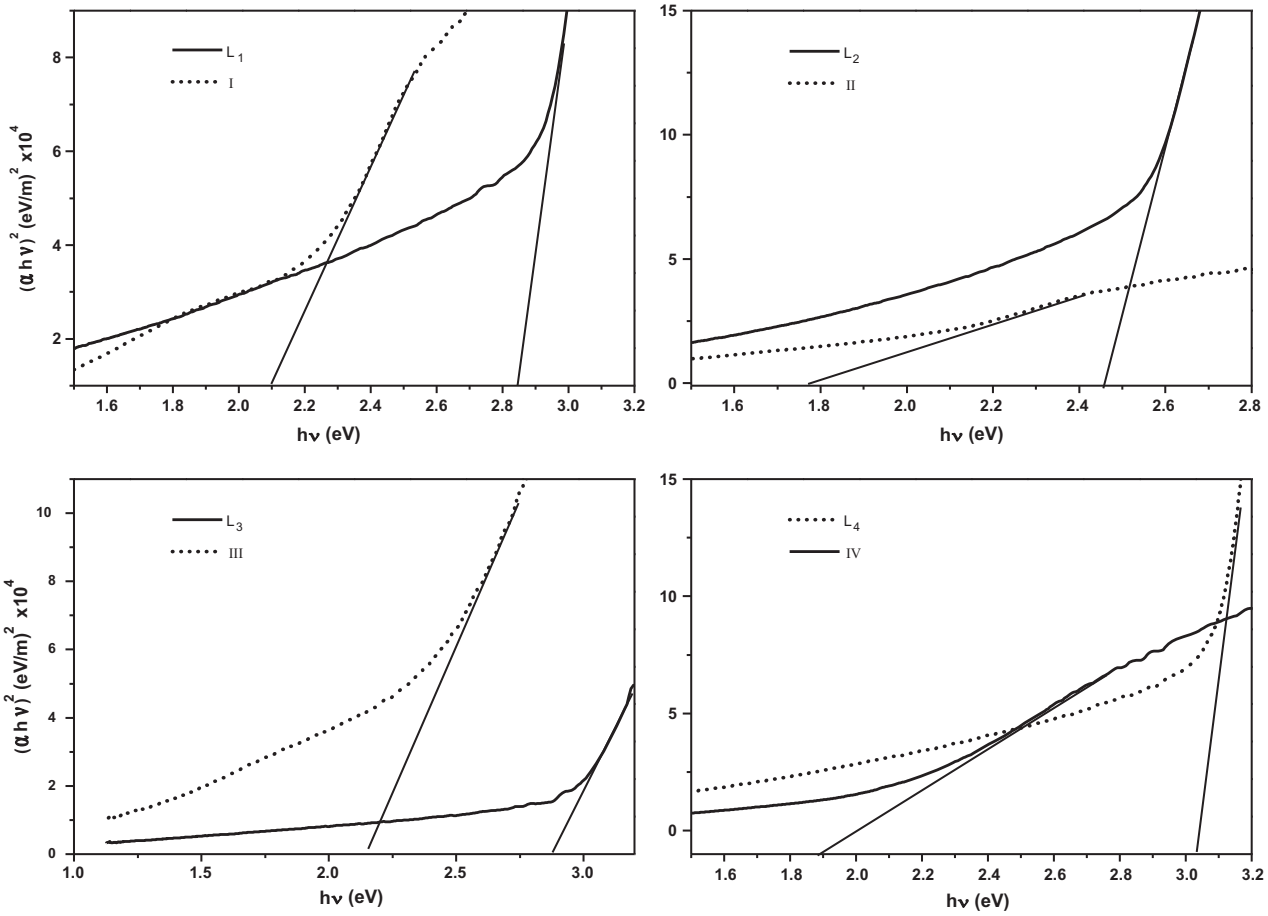

L1 = bis(salicylaldehyde)oxaloyldihydrazone, *L2 = bis(2-hydroxy-1-naphthaldehyde)oxaloyldihydrazone*

L3 = bis(2-hydroxyacetophenone)oxaloyldihydrazone, *L4 = bis(2-methoxy-benzaldehyde)oxaloyldihydrazone*

I=Cu(II)-bis(salicylaldehyde)oxaloyldihydrazone complex, *II=Cu(II)-bis(2-hydroxy-1-naphthaldehyde)oxaloyldihydrazone complex*

III = Cu(II)-bis(2-hydroxyacetophenone)oxaloyldihydrazone complex *IV = Cu(II)-bis(2-methoxy-benzaldehyde)oxaloyldihydrazone complex*

Figure 6 The plots of $(\alpha h\upsilon)^2$ vs. $h\upsilon$ of Cu^{II}-oxaloyldihydrazone complexes.

known as the hyperfine interaction. The comparable g values of **I** and **IV** may arise from the synonymous structures. The above two complexes have pseudo tetrahedral structure as indicated from the electronic absorption spectra.

In view of recorded data and from covering arguments made above, structures of the copper complexes can be represented by Fig. 5.

3.2. Optical properties

To clarify the conductivity of the isolated complexes, the optical band gap energy (E_g) of oxaloyldihydrazones and their Cu(II) complexes have been calculated from the following equations (Mott and Davis, 1979; Rashad et al., 2013; Hassan et al., 2015):

The measured transmittance (T) was used to calculate approximately the absorption coefficient (α) using the relation

$$\alpha = \frac{1}{d\ln(1/T)}$$

where d is the width of the cell and T is the measured transmittance. The optical band gap was estimated using Tauc's equation:

$$\alpha h\nu = A(h\nu - E_g)^m$$

where m is equal to 1/2 and 2 for direct and indirect transitions, respectively, and A is an energy independent constant.

The values of α calculated from the first equation were used to plot $(\alpha h\upsilon)^2$ vs. $h\upsilon$ (Fig. 6) from which an indirect band gap was found by extrapolating the linear portion of the curve to $(\alpha h\upsilon)^2 = 0$. The values of indirect optical band gap E_g were determined and are given in Table 2. The E_g values of oxaloyldihydrazones (**L_1–L_4**) and Cu(II)-L complexes were found to be at 3.06–3.42 and 1.78–2.12 eV, respectively as indicated in Fig. 6 and Table 2. Inspection of Table 2 revealed higher E_g values of ligands compared with their corresponding complexes. As reported in the literature (Karipcin et al., 2007) it is suggested that after complexation, metal tends to raise mobilization of the ligand electrons by accepting them in its shell. It can be evaluated that after formation of the complex,

Please cite this article in press as: Ahmed, A.H. et al., Copper(II)-oxaloyldihydrazone complexes: Physico-chemical studies: Energy band gap and inhibition evaluation of free oxaloyldihydrazones toward the corrosion of copper metal in acidic medium. Arabian Journal of Chemistry (2016), http://dx.doi.org/10.1016/j.arabjc.2016.05.015

the chemical structure of the ligands is changed, the width of the localized levels is expanded and in turn, the band gap is smaller. This result is very significant in applications of electronic and optoelectronic devices, because of the lower optical band gap of the materials (Turan et al., 2014). Worthy mention, small band gap facilitates electronic transitions between the HOMO–LUMO energy levels and makes the molecule more electro-conductive (Sengupta et al., 1998). The obtained band gap values suggest that these complexes are semiconductors and lie in the same range of highly efficient photovoltaic materials. So, the present compounds could be considered potential materials for harvesting solar radiation in solar cell applications (Fu et al., 2005). The little difference in the optical band gap E_g values between all studied complexes may be due to their synonymous chemical structures.

3.3. Corrosion inhibition of ligands

Weight loss data of copper in 1 M HCl in the absence and presences of various concentrations of inhibitors were obtained and are given in Fig. 7. It is obvious from this table that the weight loss decreases as the concentrations of different compounds increase. Also, it was observed that inhibition efficiencies increase with increase in inhibitor concentrations. This behavior resulted from the adsorption of hydrazones on the metal coupons/solution interface where the adsorbed species mechanically screen the coated part of the metal surface from the action of the corrosive medium. This adsorption could be attributed to physico-chemical properties of the investigated ligands molecules as functional groups (OH, NH, C═O and C═N), quite large molecular size, high molecular weight, aromaticity, electron density at the donor atoms (N:,:O:) and also the π-orbital character of azomethine, carbonyl and phenyl groups. Adsorption and desorption of inhibitor molecules continuously occur at the metal surface and an equilibrium exists between the two processes at a particular temperature. The inhibition efficiencies of hydrazones are arranged in the sequence $\mathbf{L_4} > \mathbf{L_3} > \mathbf{L_1} > \mathbf{L_2}$ and this trend can be interpreted as follows. The difference in the inhibition efficiencies of the four compounds lies in their steric factor and electron density at the donor atoms. Nevertheless, all hydrazone ligands are capable to attach to the metal surface, the persistence of methoxy (OMe) group in (L_4) which is an efficient electron donating group than phenolic-OH group present in other compounds

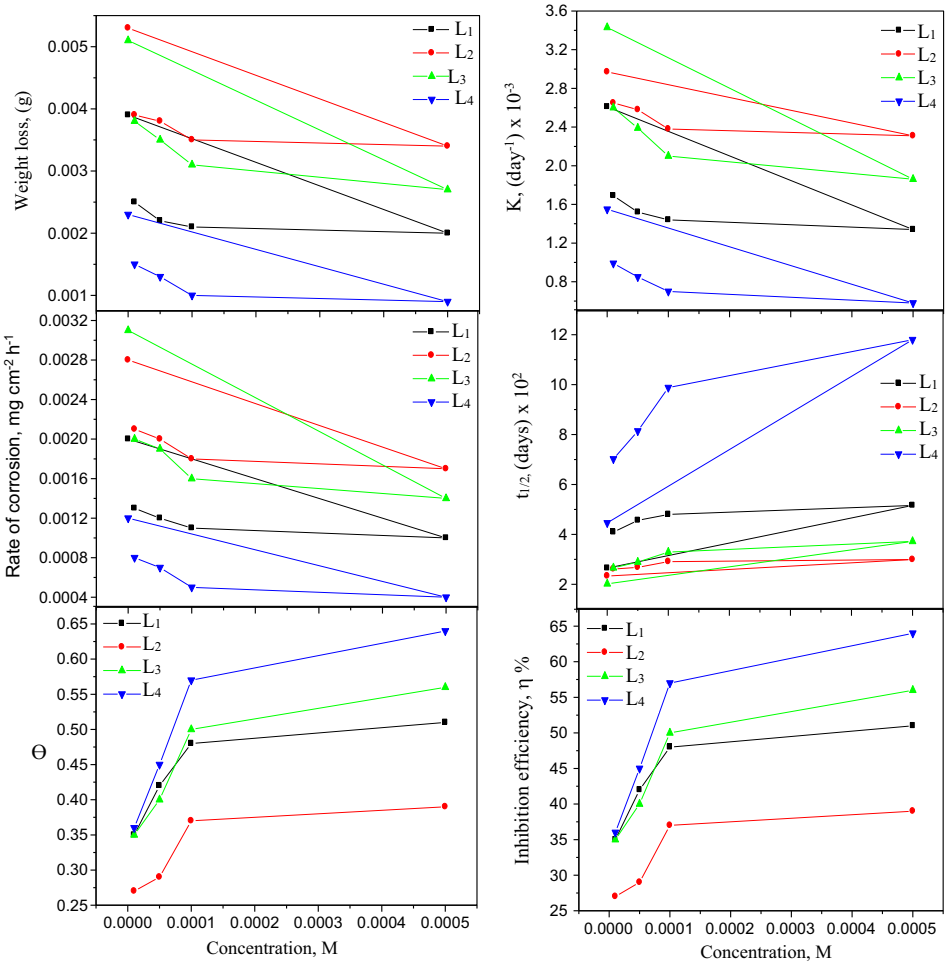

L₁ = bis(salicylaldehyde)oxaloyldihydrazone, *L₂ = bis(2-hydroxy-1-naphthaldehyde)oxaloyldihydrazone*

L₃ = bis(2-hydroxyacetophenone)oxaloyldihydrazone, *L₄ = bis(2-methoxy-benzaldehyde)oxaloyldihydrazone*

Figure 7 Corrosion parameters for copper coupons in (1 M HCl) solution in presence and absence of different concentrations of hydrazone ligands.

Please cite this article in press as: Ahmed, A.H. et al., Copper(II)-oxaloyldihydrazone complexes: Physico-chemical studies: Energy band gap and inhibition evaluation of free oxaloyldihydrazones toward the corrosion of copper metal in acidic medium. Arabian Journal of Chemistry (2016), http://dx.doi.org/10.1016/j.arabjc.2016.05.015

facilitates the adsorption on the metal surface. Positive mesomeric effect (+M effect) and negative inductive effect (−I effect) of −OCH_3 lead to increase the electron density at phenyl ring which pushes the electrons toward the donor atoms in O=C−NH−N=CH part by virtue of resonance and subsequently enhances the bond strength between the molecule and the corroding metal (Hassan et al., 2015). Under these circumstances, the inhibition efficiency of (**L_4**) should be higher than that of other ligands. **L_3** comes after L_4 due to the electron donating nature of methyl group attached to the azomethine (−N=C(CH_3)) which increases the electron density on the azomethine group causing high bond strength between ligand and metal surface. Perhaps, **L_1** comes before **L_2** because the electron pair on the ortho-OH group reaches directly to the azomethine group upon delocalization with one phenyl ring while in case **L_2** the existence of two naphthyl rings at each side of molecule may cause crowding (steric factor) that encourages incomplete coating besides they can pull or withdraw the electron pair from the ortho-OH group to themselves under the resonance effect. The order of increasing inhibition efficiency of the hydrazide derivatives is depicted in Fig. 7 for copper in 1 M HCl. The obtained data, Fig. 6, indicate a clue for the application of the used ligands especially **L_4** as corrosion inhibitors. The obtained maximum efficiency for **L_4** is 64% for copper, which indicates an acceptable inhibition for copper. Worthy mention, the inhibition efficiency values are not extremely high owing to the lower ligand concentrations.

3.3.1. Kinetic considerations

Regarding the experimental section, when log W_f was plotted against time, Fig. 8, for copper sheets in the presence of oxaloyldihydrazone ligands, a linear variation was observed, which indicated first-order reaction kinetics with respect to the abovementioned sheet in HCl solutions (Hassan et al., 2015). Fig. 7 gives the rate constants and half-life values. There is a general decrease in the rate constants with increasing concentrations of oxaloyldihydrazone inhibitors (L_1–L_4), Fig. 7. The enhancement of half-life ($t_{1/2}$) with increase in concentration of hydrazone ligands sustains the inhibition of the copper in 1 M HCl by the additives. The increase in half-life reflects more protection of the metals by the oxaloyldihydrazone ligands (Hassan et al., 2015).

3.3.2. Adsorption isotherms and Gibb's free energy

Values of θ, degree of surface coverage, calculated from weight loss measurements have been used to study the adsorption characteristics of the inhibitors on the surface of copper metal. The data obtained at room temperature (nearby 303 K) were tested to fit curves for different adsorption isotherms including Freundlich, Temkin, Langmuir, Frumkin and Flory–Huggins, and the correlation coefficients (R^2) were used to determine the best fits. The Gibb's free energy of adsorption ΔG_{ads} at room temperature for all tested isotherms was calculated according to the following relation (Rodosevic et al., 1995):

$$\Delta G_{ads.} = -RT55.5K_{ads.}, \quad \text{where } T \text{ is the temperature (in K)}$$

3.3.2.1. Freundlich isotherm. Freundlich isotherm is given by the relation (Mohammad et al., 2011)

$$\ln\theta = \ln K_{ads.} + \frac{1}{n}\ln C$$

where C is the inhibitor bulk concentration in mol/L, $K_{ads.}$ (mol^{-1} L) is the equilibrium constant of adsorption and n is Freundlich heterogeneity factor.

Fig. 8 shows the plot of surface coverage θ versus logarithmic concentration of all ligands. The linear plot with acceptable correlation coefficient was obtained indicating that the adsorption of the inhibitors onto different metal surfaces can be described by Freundlich isotherm. The adsorption parameters obtained for Freundlich adsorption isotherm are shown in Fig. 10. In the present study for different inhibitors, n values are greater than unity implying favored adsorption process (Ahmad et al., 2005).

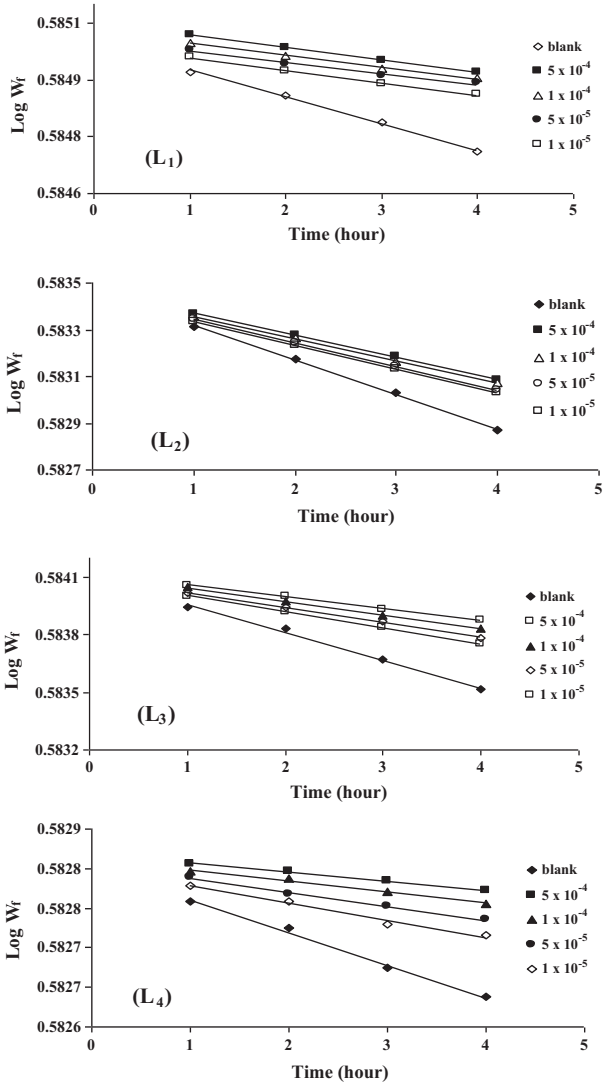

L_1 = bis(salicylaldehyde)oxaloyldihydrazone,
L_2 = bis(2-hydroxy-1-naphthaldehyde)oxaloyldihydrazone
L_3 = bis(2-hydroxyacetophenone)oxaloyldihydrazone,
L_4 = bis(2-methoxy-benzaldehyde)oxaloyldihydrazone

Figure 8 Variation of log W_f with time for copper coupons in HCl solution containing oxaloyldihydrazones.

Please cite this article in press as: Ahmed, A.H. et al., Copper(II)-oxaloyldihydrazone complexes: Physico-chemical studies: Energy band gap and inhibition evaluation of free oxaloyldihydrazones toward the corrosion of copper metal in acidic medium. Arabian Journal of Chemistry (2016), http://dx.doi.org/10.1016/j.arabjc.2016.05.015

3.3.2.2. Langmuir adsorption. This isotherm may be formulated as (Shockry et al., 1998)

$$\frac{C}{\theta} = \frac{1}{K} + C$$

where K is the equilibrium constant for adsorption process.

Fig. 9 represents the plot of $\log C/\theta$ versus $\log C$ for different compounds relative to copper metal. The obtained linear plots with high correlation coefficients indicate that the adsorption of the inhibitors onto different metal surface follows Langmuir adsorption isotherm. From the resulting data one can postulate that there is no interaction between the adsorbed species. The thermodynamic parameters for adsorption process, K_{ads} and ΔG_{ads}, associated with the investigated compounds are displayed in Fig. 10.

3.3.2.3. Frumkin adsorption. Frumkin adsorption isotherm is given by Eddy et al. (2008)

$$\log C\left[\frac{\theta}{1-\theta}\right] = 2.303 \log K + 2\alpha\theta$$

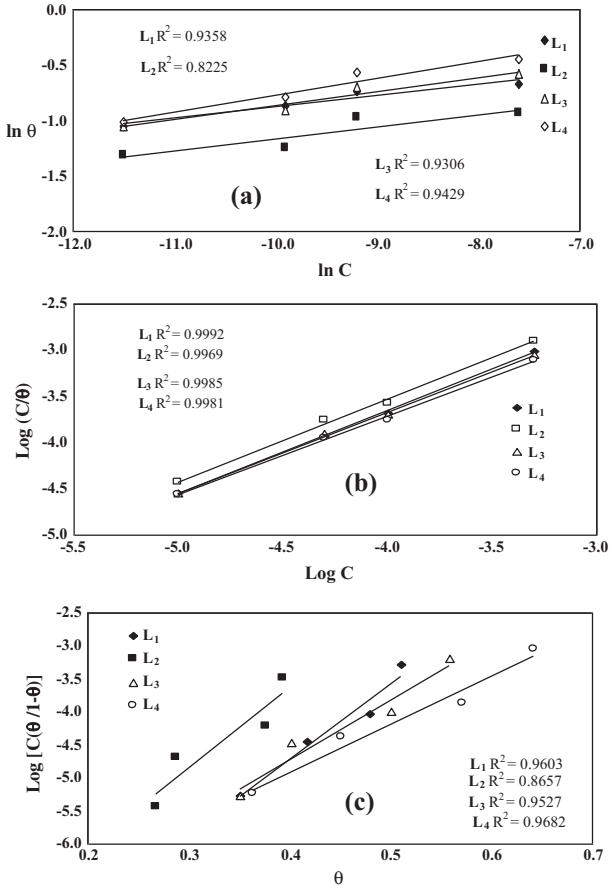

L1 = bis(salicylaldehyde)oxaloyldihydrazone,
L2 = bis(2-hydroxy-1-naphthaldehyde)oxaloyldihydrazone
L3 = bis(2-hydroxyacetophenone)oxaloyldihydrazone,
L4 = bis(2-methoxy-benzaldehyde)oxaloyldihydrazone

Figure 9 Plots of (**a**) Freundlich $\ln\theta$ vs. $\ln C$, (**b**) Langmuir Log (C/θ) vs. Log C, and (**c**) Frumkin Log $C[\theta/(1-\theta)]$ vs. θ for copper coupons in HCl solution containing oxaloyldihydrazones.

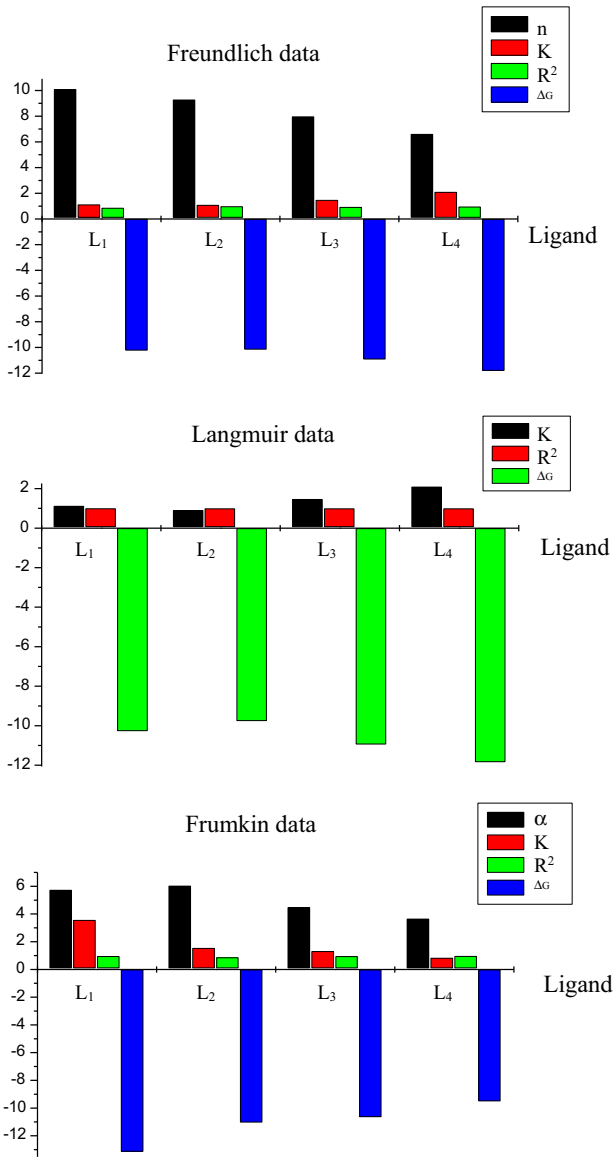

L1 = bis(salicylaldehyde)oxaloyldihydrazone,
L2 = bis(2-hydroxy-1-naphthaldehyde)oxaloyldihydrazone
L3 = bis(2-hydroxyacetophenone)oxaloyldihydrazone,
L4 = bis(2-methoxy-benzaldehyde)oxaloyldihydrazone

Figure 10 Values of ΔG_{ads} (kJ/mol), adsorption constant (K), Freundlich heterogeneity factor (n), lateral interaction term describing the interaction in adsorbed layer (α), and correlation coefficient (R^2) of inhibitors for copper coupons.

where K is the adsorption–desorption constant and α is the lateral interaction term describing the interaction in adsorbed layer.

Plots of $\log C[\theta/(1-\theta)]$ against θ as presented in Fig. 9 were linear with acceptable correlation coefficients suggesting the applicability of Frumkin isotherm. The values for Frumkin adsorption parameters are represented in Fig. 10. The results gave positive α values suggesting the attractive behavior of the inhibitor on the surface of copper (Ashassi-Sorkhabi et al., 2006).

Please cite this article in press as: Ahmed, A.H. et al., Copper(II)-oxaloyldihydrazone complexes: Physico-chemical studies: Energy band gap and inhibition evaluation of free oxaloyldihydrazones toward the corrosion of copper metal in acidic medium. Arabian Journal of Chemistry (2016), http://dx.doi.org/10.1016/j.arabjc.2016.05.015

3.3.3. Adsorption consideration

The inhibition effect of inhibitor compound is ascribed to adsorption of the molecule on metal surface. This adsorption may be physical or chemical depending on the adsorption strength. For a physical adsorption mechanism, the value of the free energy (ΔG_{ads}) of adsorption should be less negative than −40 kJ/mol. The negative values of ΔG_{ads} set out in Fig. 10 suggest spontaneous adsorption of the inhibitor and characterize their strong interaction with the metal surface (Bilgic and Sahin, 2001). The magnitudes of ΔG_{ads}(> −40 kJ/mol) indicate that adsorption on metal surface is compatible with physical adsorption mechanism (Bilgic and Sahin, 2001). Accordingly, the corrosion inhibition may be justified due to the formation of a protective film on the metal surface where the additive covered both the anodic and cathodic sites.

4. Summary and conclusion

A series of copper(II)-hydrazone complexes derived from selected oxaloyldihydrazones (**L_1**–**L_4**) have been isolated in pure form. All the ligands and their four solid copper(II) complexes can be prepared by traditional reflux method. Comparison of the elemental analysis for both calculated and found percentages indicates that the compositions of the isolated solid complexes coincide well with the proposed formulae. Elemental analyses (C, H, N and M%), (FT-IR, UV–Vis, ESR) spectroscopy, thermal measurement, magnetism at room temperature besides the difference in the color between the free ligand and its relevant complex evidenced the formation of the desired copper-hydrazone complexes. The copper ions tend to give binuclear complexes with all ligands. The indirect band gap energy value (E_g) of ligands and their relevant complexes is considered a characteristic feature of semiconductor materials. On the basis of various physico-chemical data presented and discussed above, the complexes may tentatively be suggested to have trigonal distorted octahedral (**I**) and pseudo tetrahedral (**II**–**IV**) configurations. The indirect band gap energy (E_g) for all separated compounds lies in the range of semiconductor materials. The results of corrosion inhibition presented in this work point to the ability of all ligands to inhibit the corrosion of copper in HCl solution. The inhibition efficiencies of the inhibitors increase with increasing the inhibitor concentration following the descending order: **L_4 > L_3 > L_1 > L_2**. The obtained values of Gibb's free energy are attributed to physical adsorption of the ligands on the copper surface. The experimental data coincide well with Freundlich, Langmuir and Frumkin adsorption isotherms for all investigated oxaloyldihydrazone inhibitors.

References

Abd El-Wahab, H., Abd El-Fattah, M., Ahmed, A.H., Elhenawy, A. A., Alian, N.A., 2015. J. Organomet. Chem. 791, 99–106.
Ahmad, A.L., Bhatia, S., Ibrahim, N., Sumathi, S., 2005. Braz. J. Chem. Eng. 22, 1–13.
Ahmed, A.H., 2014. Rev. Inorg. Chem. 34 (3), 153–175.
Ahmed, A.H., Hassan, A.M., Gumaa, H.A., Mohamed, B.H., Eraky, A.M., 2015. J. Adv. Chem. 11 (10), 3834–3847.
Ashassi-Sorkhabi, H., Shaabani, B., Aligholipour, B., Seifzadeh, D., 2006. Appl. Surf. Sci. 252, 4039–4047.
Barbazan, P., Carballo, R., Covelo, B., Lodeiro, C., Lima, J.C., Vazquez-Lopez, E.M., 2008. Eur. J. Inorg. Chem., 2713–2720
Berger, S.A., 1979. Mikrochim. Acta 71 (3–4), 311–316.
Berger, S.A., 1993. Microchem. J. 47 (3), 317–324.
Berger, S.A., Ryan, D.E., 1974. Mikrochim. Acta 62 (4), 679–688.
Bilgic, S., Sahin, M., 2001. Mater. Chem. Phys. 70, 290–295.
Eddy, N.O., Odoemelam, S.A., 2008. J. Surface Sci. Technol. 24 (1–2), 1–14.
Eddy, N.O., Ekwumemgbo, P., Odoemelam, S.A., 2008. Int. J. Phys. Sci. 3, 1–6.
Flick, E.W., 1987. Corrosion Inhibitors. Park Ridge, New Jersey.
Fu, M.L., Guo, G.C., Liu, X., Cai, L.Z., Huang, J.S., 2005. Inorg. Chem. Commun. 8, 18–21.
Hassan, A.M., Ahmed, A.H., Mohamed, T.A., Mohamed, B.H., 2007. Trans. Met. Chem. 32, 461–467.
Hassan, A.M., Ahmed, A.H., Gumaa, H.A., Mohamed, B.H., Eraky, A.M., 2015. J. Chem. Pharm. Res. 7 (7), 91–104, and references therein.
Karipcin, F., Dede, B., Caglar, Y., Hur, D., Ilican, S., Caglar, M., Sahin, Y., 2007. Opt. Commun. 272, 131–137.
Kivelson, D., Nieman, R., 1961. J. Chem. Phys. 35, 149–155.
Kumar, A., Lal, R.A., Chanu, O.B., Borthakur, R., Koch, A., Lemtur, A., Adhikari, S., Choudhury, S., 2011. J. Coord. Chem. 64 (10), 1729–1742.
Lal, R.A., Adhikari, S., Kumar, A., Chakraborty, J., Bhaumik, S., 2002. Synth. React. Inorg. Met.-Org. Chem. 32 (1), 81–96.
Lal, R.A., Basumatary, D., Adhikari, S., Kumar, A., 2008. Spectrochim. Acta A 69 (3), 706–714.
Lal, R.A., Basumatary, D., Adhikari, S., Kumar, A., 2008. Spectrochim. Acta Part A Mol. Biomol. Spectrosc. 69 (3), 706–714.
Lever, A.B.P., 1984. Inorganic Electronic Spectroscopy. Elsevier Publishing Company, Amsterdam.
Lopez-Sesenes, R., Gonzalez-Rodriguez, J.G., Casales, M., Martinez, L., Sanchez-Ghenno, J.C., 2011. Int. J. Electrochem. Sci. 6, 1772–1784.
Lorenz, W.J., Mansfield, F., 1985. In: Proceedings of the 6th Symposium on European Inhibition of Corrosion, University of Ferrara, Ferrara, 23 (available at sciencedirect.com).
Mahapatra, B.B., Kar, S.K., 1991. J. Ind. Chem. Soc. 68, 542–544.
Mohammad, R., Hadj, M., Mina, S., Pourya, B., 2011. J. Appl. Sci. Environ. Sanit. 6, 1–13.
Mohammed-Dabo, I.A., Yaro, S.A., Abubakar, G., Ayilara, S.I., Apugo-Nwosu, T.U., Akuso, S.A., 2011. J. Basic. Appl. Sci. Res. 1, 1989–1999.
Mott, N.F., Davis, E.A., 1979. Electronic Processes in Non-Crystalline Materials, second ed. Clarendon Press, Oxford.
Nakamoto, K., 1970. Inorganic Spectra of Inorganic and Coordination Compounds, second ed. John Wiley & Sons, New York.
Odashima, T., Anzai, F., Ishii, H., 1976. Anal. Chim. Acta 86, 231–236.
Okafor, P.C., Ebenso, E.E., Ekpe, U.J., 2010. Int. J. Electrochem. Sci. 5, 978–993.
Orubite-Okorosaye, K., Oforka, N.C., 2004. J. Appl. Sci. Environ-Manage. 8 (1), 57–61.
Rashad, M.M., Hassan, A.M., Nassar, A.M., Ibrahim, N.M., Mourtada, A., 2013. Appl. Phys. A 117, 877–890.
Rodosevic, J., Kliskic, M., Aljinovic, L.J., Vuko, S., 1995. In: The Proceedings of the 8th European Symposium on Corrosion Inhibition, Ann Univ., Ferrara, Italy, p. 817.
Rollas, S., Kucukguzel, S.G., 2007. Molecules 12 (8), 1910–1939.
Salama, T.M., Ahmed, A.H., El-Bahy, Z.M., 2006. Micropor. Mesopor. Mater. 89, 251–259.
Salapathy, S., Sahoo, B., 1970. J. Inorg. Nucl. Chem. 32 (7), 2223–2227.
Salavati-Niasari, M., Sobhani, A., 2008. J. Mol. Catal. A: Chem. 285, 58–67.

Please cite this article in press as: Ahmed, A.H. et al., Copper(II)-oxaloyldihydrazone complexes: Physico-chemical studies: Energy band gap and inhibition evaluation of free oxaloyldihydrazones toward the corrosion of copper metal in acidic medium. Arabian Journal of Chemistry (2016), http://dx.doi.org/10.1016/j.arabjc.2016.05.015

Sengupta, S.K., Pandey, O.P., Srivastava, B.K., Sharma, V., 1998. Transit. Met. Chem. 23, 349–353.
Sherif, E.M., Ahmed, A.H., 2010. Synth. React. Inorg. Met.-Org. Chem. 40, 365–372.
Shockry, H., Yuasa, M., Sekine, I., Issa, R.M., El-baradie, H.Y., Gomma, G.K., 1998. Corros. Sci. 40, 2173–2186.
Sutton, D., 1968. Electronic Spectra of Transition Metal Complexes. McGraw Hill, Londan.
Turan, N., Gündüz, B., Körkoca, H., Adigüzel, R., Çolak, N., Buldurun, K., 2014. J. Mex. Chem. Soc. 58 (1), 65–75.

Please cite this article in press as: Ahmed, A.H. et al., Copper(II)-oxaloyldihydrazone complexes: Physico-chemical studies: Energy band gap and inhibition evaluation of free oxaloyldihydrazones toward the corrosion of copper metal in acidic medium. Arabian Journal of Chemistry (2016), http://dx.doi.org/10.1016/j.arabjc.2016.05.015